JOURNAL OF MATERIALS SCIENCE 26 (1991) 569–578

Crack propagation in PCBA–PMMA sandwich plates

G. A. PAPADOPOULOS
Department of Engineering Science, Section of Mechanics, The National Technical University of Athens, 5 Heroes of Polytechnion Avenue, GR-157 73 Zographou, Athens, Greece

The crack propagation in PCBA (Lexan)–PMMA (Plexiglas) sandwich plates has been studied by means of the high-speed photography together with a dynamic caustics method. Various phenomena were observed in these experiments: the time lag between the two cracks propagating into the two phases of the sandwich, the time coincidence of the two propagating cracks and phenomena of acceleration, deceleration and bifurcation of the propagating cracks. More precisely, the initial crack begins to propagate first into the brittle (PMMA) phase while a second crack begins to propagate later into the ductile (PCBA) phase of the sandwich plate. The time lag and the time coincidence depend on the nature and the degree of compatibility of the two phases of the sandwich plate.

1. Introduction

Sandwich plates have been considered theoretically by many investigators. Erdogan and Arin [1] considered cracked sandwich plates and performed a mathematical evaluation of the stress intensity factors. Lee and Chang [2], in a study of the effect of thickness, stiffness and the mass of the facings on the wave propagation and vibrations in an elastic symmetrical sandwich plate, used the three-dimensional equations of elasticity.

In this paper the method of dynamic caustics [3–6], together with high-speed photography, is used to measure the crack propagation velocity, v, and the dynamic stress intensity factor, K_I^d, for sandwich plates made from polycarbonate of bisphenol A (PCBA) (Lexan) and polymethylmethacrylate (PMMA) (Plexiglas).

2. The method of dynamic caustics

The method of dynamic caustics was used to study the crack propagation behaviour in sandwich plates. In this method a convergent or divergent light beam impinges on the specimen in the vicinity of the crack tip and the transmitted rays are directed on to a reference plane parallel to the plane of the specimen. These rays are scattered and concentrated along a strongly illuminated curve, or caustic, on the reference plane located a distance z_0 from the specimen. It is then possible to calculate the stress intensity factors for mixed-mode conditions from the size and angular displacement, Φ, of the axis of symmetry of the caustic relative to the crack axis using the relations [3, 4]

$$K_I^d = \frac{2(2\pi)^{\frac{1}{2}}}{3z_0 t \lambda_m^{3/2} c_t} \left[\frac{D_t^{max}}{\delta_t^{max}(v, \xi)}\right]^{5/2} \quad (1)$$

$$K_{II}^d = K_I^d \tan\left(\frac{\Phi}{2}\right) \quad (2)$$

where z_0 is the distance between the specimen and the reference plane, t is the thickness of the specimen, λ_m is the magnification ratio of the optical set-up, c_t is the optical constant of the material, D_t^{max} is the maximum transverse diameter of the caustic and $\delta_t^{max}(v, \xi)$ is a correction factor which depends on the crack velocity, v, and the coefficient of optical anisotropy, ξ, of the birefringent materials [7, 8]. This correction factor was given by nomograms in previous publications [3, 7, 8].

3. Experimental Procedure

Notched Lexan–Plexiglas sandwich plates of area 0.3 m × 0.1 m were used for the experimental investigation. The thickness, t_L, Lexan used was 0.001, 0.0016 and 0.002 m and the thickness t_P of the Plexiglas plate was 0.001 m. The specimens initially contained an edge transverse artificial crack $a_0 = 0.01$ m as shown in Fig. 1.

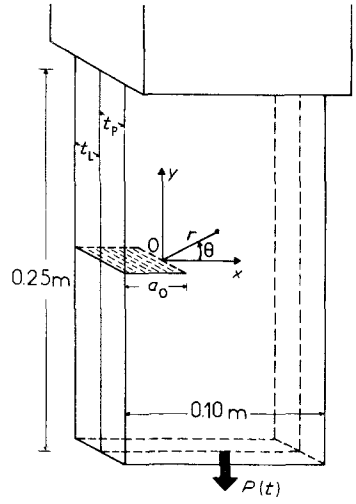

Figure 1 Geometry of the specimens.

0022–2461/91 $03.00 + .12

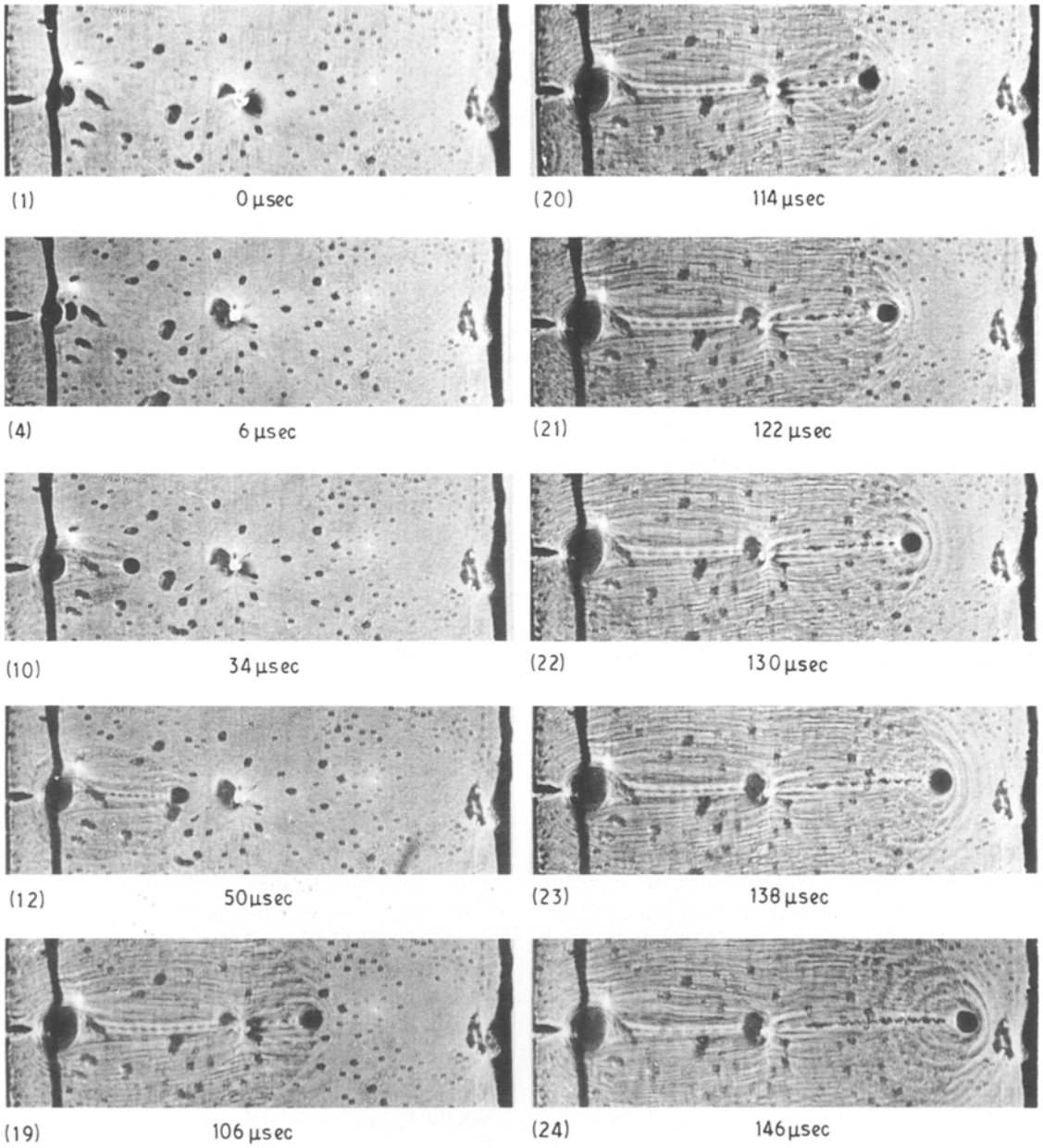

Figure 2 A series of photographs showing the crack propagation in a sandwich specimen with $t_P = 0.001$ m and $t_L = 0.0016$ m subjected to a strain rate $\dot{\varepsilon} = 24\,\text{sec}^{-1}$. The two plates were bonded with epoxy resin.

The specimens were tested to fracture under a dynamic tensile load using a hydropulse high-speed testing machine (Carl–Schenk Co.) with a maximum strain rate, $\dot{\varepsilon}$, of $80\,\text{sec}^{-1}$. A Cranz–Scharding high-speed camera dispensing 24 sparks with a maximum frequency of 10^6 frames sec^{-1} was used to record the dynamic crack propagation. In the optical set-up [3] used in the experiments, $z_0 = 0.8$ m and $\lambda_m = 0.75$. The loading strain rates, $\dot{\varepsilon}$, in the present work were 4, 8, 24 and $40\,\text{sec}^{-1}$. The optical constant [9] for the Plexiglas was $c_t^{(P)} = 0.74 \times 10^{-10}\,\text{m}^2\,\text{N}^{-1}$ and for the Lexan was $c_t^{(L)} = 1.55 \times 10^{-10}\,\text{m}^2\,\text{N}^{-1}$.

4. Results and discussion

In order to study the behaviour of dynamic crack propagation in sandwich plates, a number of specimens consisting of two materials bonded together were fractured at various strain rates. Fig. 1 shows the geometry of the specimens. The specimens consisted of a Plexiglas plate and a Lexan plate which were bonded using either epoxy resin or the adhesive cement trichloroethylene–dichloromethane (2/1).

The detailed crack propagation process can be studied using a series of photographs taken with a Cranz–Schardin high-speed camera. Fig. 2 presents such a series showing the crack propagation in a sandwich specimen consisting of a Plexiglas plate ($t_P = 0.001$ m) and a Lexan plate ($t_L = 0.0016$ m) bonded with epoxy resin. This specimen was subjected to a strain rate $\dot{\varepsilon} = 24\,\text{sec}^{-1}$. The photographs show clearly that crack propagation starts in the Plexiglas plate but is not observed in the Lexan plate because debonding takes place around the propagating crack. This implies that the adhesion between the plates and the epoxy resin phase was poor. Crack propagation starts in the Lexan plate after the exit of the crack from the Plexiglas plate. Frame 24 of Fig. 2 shows that crack propagation has not yet begun in the Lexan plate. The caustic at the initial crack-tip is double and

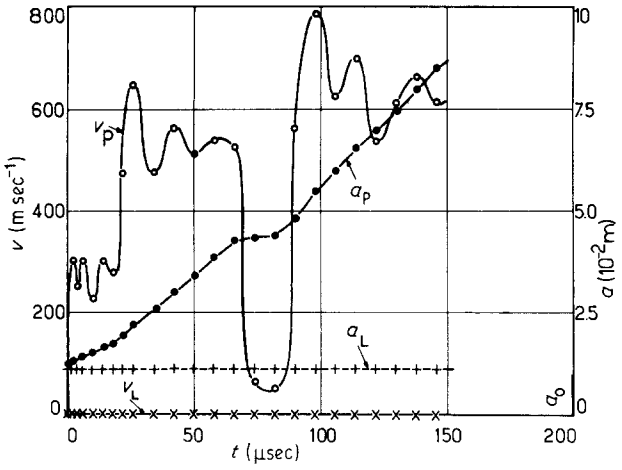

Figure 3 Variation in the crack propagation velocity, v, and the crack length, a, in (○, ●) the Plexiglas and (× , +) the Lexan plate of the sandwich specimen, with the propagation time, t, for the specimen in Fig. 2.

greater than the caustic in the Plexiglas plate. This means that this crack is in the Lexan plate [7].

The crack propagation velocities, v_P and v_L, and the crack lengths, a_P and a_L, in the Plexiglas and Lexan plates are plotted against time, t, in Fig. 3. The crack velocity, v_P, in the Plexiglas plate reaches high values, but the crack velocity, v_L, in the Lexan plate remains zero. At $t \simeq 80$ μsec, a minimum is observed in v_P because the crack entered a region with good adhesion between the plates and the epoxy resin phase and so the crack propagation decelerated. The dynamic stress intensity factor, K_I^d, in the Plexiglas and Lexan plates is plotted against time, t, in Fig. 4. The stress intensity factor in the Lexan plate reaches high values. This stress intensity factor is static because the crack is not propagating.

Fig. 5 shows similar results to those presented in Fig. 2. The adhesion between the plates and the epoxy resin phase is better than in the specimen used in Fig. 2. Of course, a weaker debonding than in the Fig. 2 takes place around the propagating cracks. Crack propagation started in the Plexiglas plate and

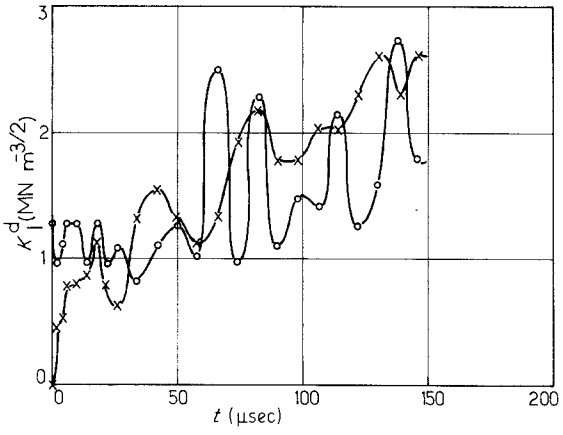

Figure 4 Variation in the dynamic stress intensity factor, K_I^d, in (○) the Plexiglas and (×) the Lexan plate of the sandwich specimen, with the propagation time, t, for the specimen in Fig. 2.

was followed about 30 μsec later (time lag) by propagation in the Lexan plate. The time lag of 30 μsec depends on the nature and degree of compatibility of the two plates. The crack velocities, v_P and v_L, and the crack lengths, a_P and a_L, in the Plexiglas and Lexan plates are plotted against time, t, in Fig. 6. Acceleration, decceleration and crack bifurcation phenomena can be observed in both plates in this experiment (frames 16 and 17, Fig. 5). The dynamic stress intensity factor, K_I^d, in the Plexiglas and Lexan plates is plotted against time, t, in Fig. 7.

Fig. 8 presents a series of photographs showing the crack propagation in a sandwich specimen consisting of a Plexiglas plate ($t_P = 0.001$ m) and a Lexan plate ($t_L = 0.002$ m) bonded with adhesive cement trichloroethylene–dichloromethane (2/1) so that there was no other phase between the two plates. The adhesion was good. This specimen was subjected to a strain rate $\dot{\varepsilon} = 4\ \text{sec}^{-1}$. The photographs show that crack propagation starts in the Plexiglas plate (small caustic) while the caustic at the crack tip in the Lexan plate increases but crack propagation is not observed. The time lag between the two propagating cracks is longer than the 352 μsec. So, the nature of the Lexan and its thickness influence very strongly the crack propagation in the brittle material, Plexiglas, for static or quasi-static loading. In this experiment, the Lexan plate does not allow high initiation velocities of cracks in the brittle Plexiglas plate. As is seen in Figs 9 and 10, the crack propagation velocity of the crack and the stress intensity factor, K_I^d, respectively, in Plexiglas plate are very low.

Fig. 11 presents a series of photographs showing the crack propagation in a sandwich specimen similar to that of Fig. 8 but with strain rate $\dot{\varepsilon} = 8\ \text{sec}^{-1}$. As it appears, the adhesion was very good and the degree of compatibility was high, and no debonding of the two plates during crack propagation was observed. As can be seen in this figure, the crack initiated in both plates but with different velocities and with a time lag shorter than the 8 μsec (because the time between frames is 8 μsec). After about 88 μsec (frame 12, Fig. 11) the two propagating cracks met and then propagated as a single crack. The crack velocities v_P and v_L and the crack lengths a_P and a_L are plotted against time, t, in Fig. 12. It can be seen that the crack in the Lexan plate accelerates and the crack in the Plexiglas plate decelerates until the two cracks coincide after about 88 μsec. The variation of the dynamic stress intensity factor, K_I^d, in the Plexiglas and Lexan plates is plotted against time, t, in Fig. 13. It can be observed that the values of the stress intensity factor in Plexiglas plate were strongly influenced by the Lexan plate.

Fig. 14 shows similar results to those presented in Fig. 11 but with a strain rate $\dot{\varepsilon} = 24\ \text{sec}^{-1}$. It can be observed that after about 60 μsec the two propagating cracks met and then propagated as a single crack which, after 72 μsec, bifurcated (frame 11, Fig. 14). It can be seen in Fig. 15 that the crack accelerates and decelerates in Plexiglas (v_P) and Lexan (v_L) plate, respectively. Fig. 16 shows the variation and the interaction of the stress intensity factors in the two plates of the sandwich.

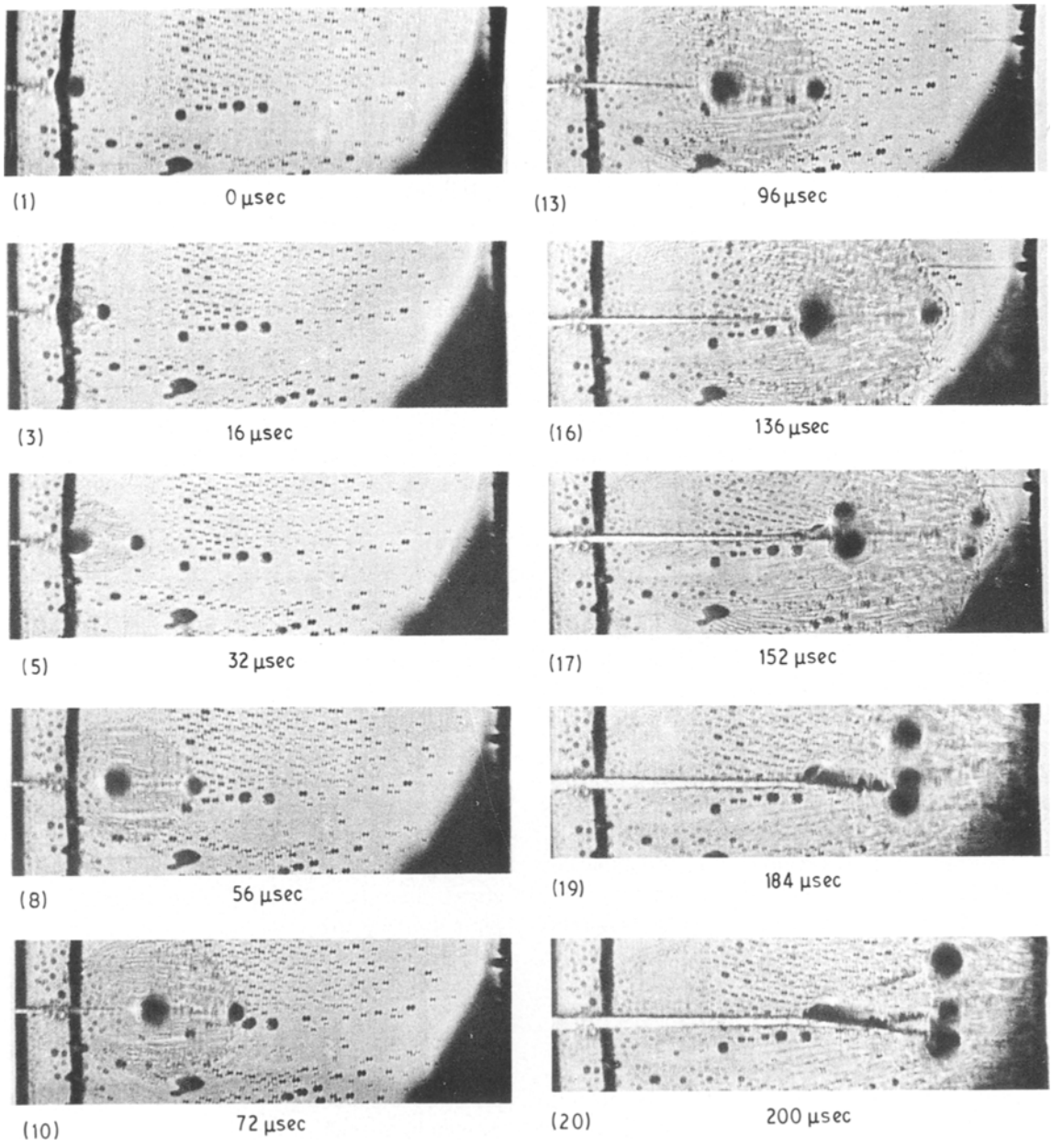

Figure 5 A series of photographs showing the crack propagation in a sandwich specimen with $t_P = 0.001$ m and $t_L = 0.0016$ m subjected to a strain rate $\dot{\varepsilon} = 24\ \text{sec}^{-1}$. The two plates were bonded with epoxy resin.

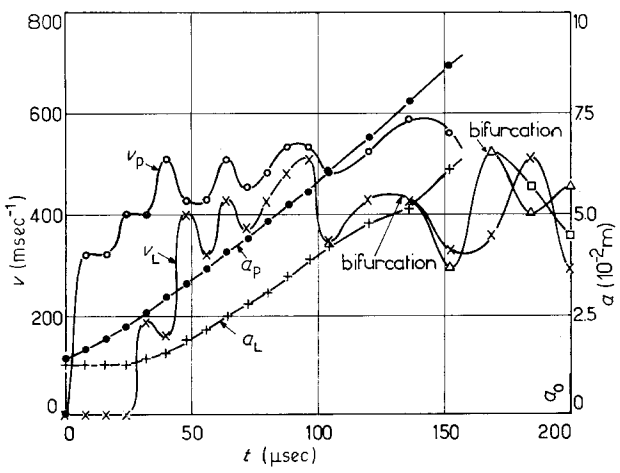

Figure 6 Variation in the crack velocity, v, and the crack length, a, with time, t, for the specimen in Fig. 5. (○, ●) Plexiglas, (× , + , △, □) Lexan.

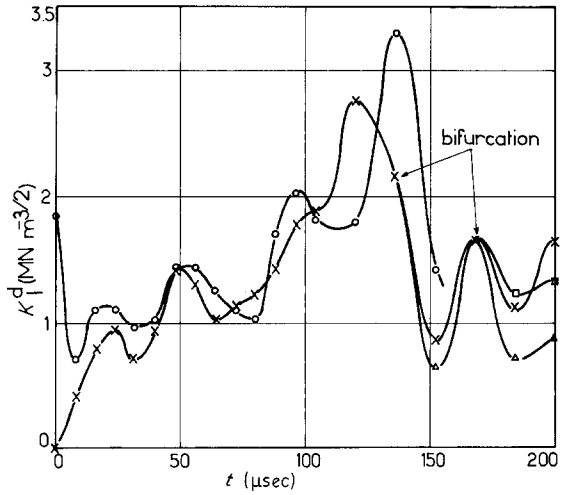

Figure 7 Variation in K_I^d with time, t, for the specimen in Fig. 5. (○) Plexiglas, (× , △, □) Lexan.

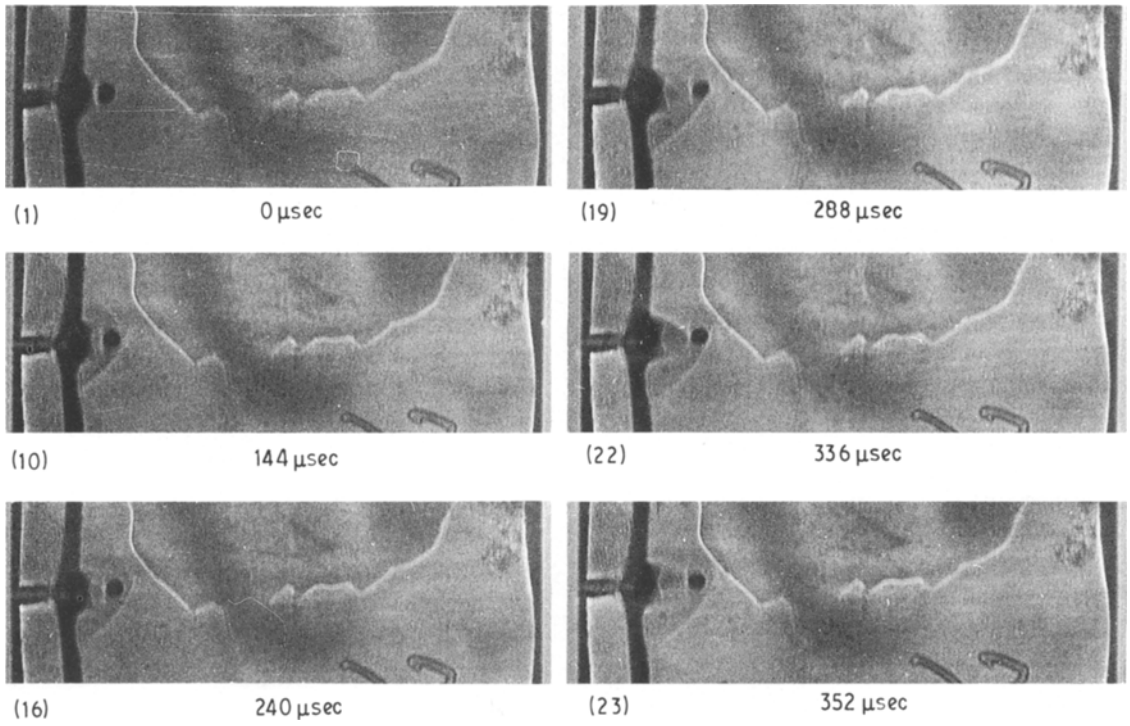

Figure 8 A series of photographs showing the crack propagation in a sandwich specimen with $t_P = 0.001$ m and $t_L = 0.002$ m subjected to a strain rate $\dot{\varepsilon} = 4\ \text{sec}^{-1}$. The two plates were bonded with the adhesive cement trichloroethylene–dichloromethane.

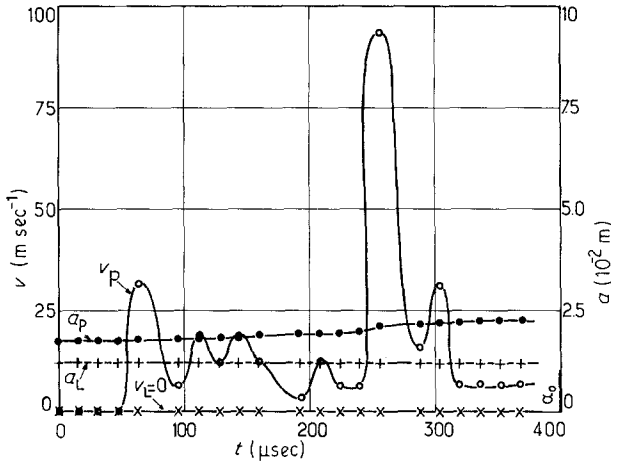

Figure 9 Variation in the crack velocity, v, and the crack length, a, with time, t, for the specimen in Fig. 8. (●, ○) Plexiglas, (+ , ×) Lexan.

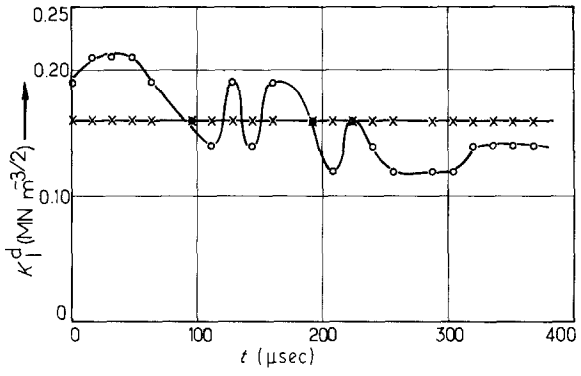

Figure 10 Variation in K_I^d with time, t, for the specimen in Fig. 8. (○) Plexiglas, (×) Lexan.

Fig. 17 shows similar results to those of Figs 11 and 14 but with strain rate $\dot{\varepsilon} = 40\ \text{sec}^{-1}$. The time lag is shorter than the 4 μsec (the time between frames is 4 μsec). The coincidence time (t_{coin}) of the two propagating cracks is about 40 μsec (frame 12, Fig. 17). After about 60 μsec a bifurcation is observed. The variation of the crack velocities (v_P, v_L) and the crack lengths (a_P, a_L), as well as the variation of the stress intensity factors in two plates of the sandwich, are presented in Figs 18 and 19, respectively.

In order to present the influence of the thickness of the ductile plate (Lexan) on to crack propagation in the brittle phase (Plexiglas) a number of sandwich specimens with the same thickness of plates was fractured at difference strain rates. So, Figs 20 and 21 show the variation of the crack velocities (v_P, v_L) and the crack lengths (a_P, a_L) and the stress intensity factor, K_I^d with time, t, respectively, for a sandwich specimen with the same plates thicknesses, $t_P = t_L = 0.001$ m. The strain rate was $\dot{\varepsilon} = 4\ \text{sec}^{-1}$. It can be seen that the time lag is zero. This means that at the same time crack propagation occurs in both plates of the sandwich, thus the propagating crack was single, because the two crack-tips were coincident.

Figs 22 and 23 show the variation of the crack velocities and crack lengths and the stress intensity factor with the time, t, respectively, for a sandwich specimen with $t_P = t_L = 0.001$ m which fractured at a strain rate of $\dot{\varepsilon} = 8\ \text{sec}^{-1}$. In this experiment, a short time lag and a $t_{coin} \simeq 45$ μsec were observed. It can be seen that the values of velocities and the values of the stress intensity factor in comparison with those in Figs 12 and 13 mainly remain smaller than those for the values in the Plexiglas plate.

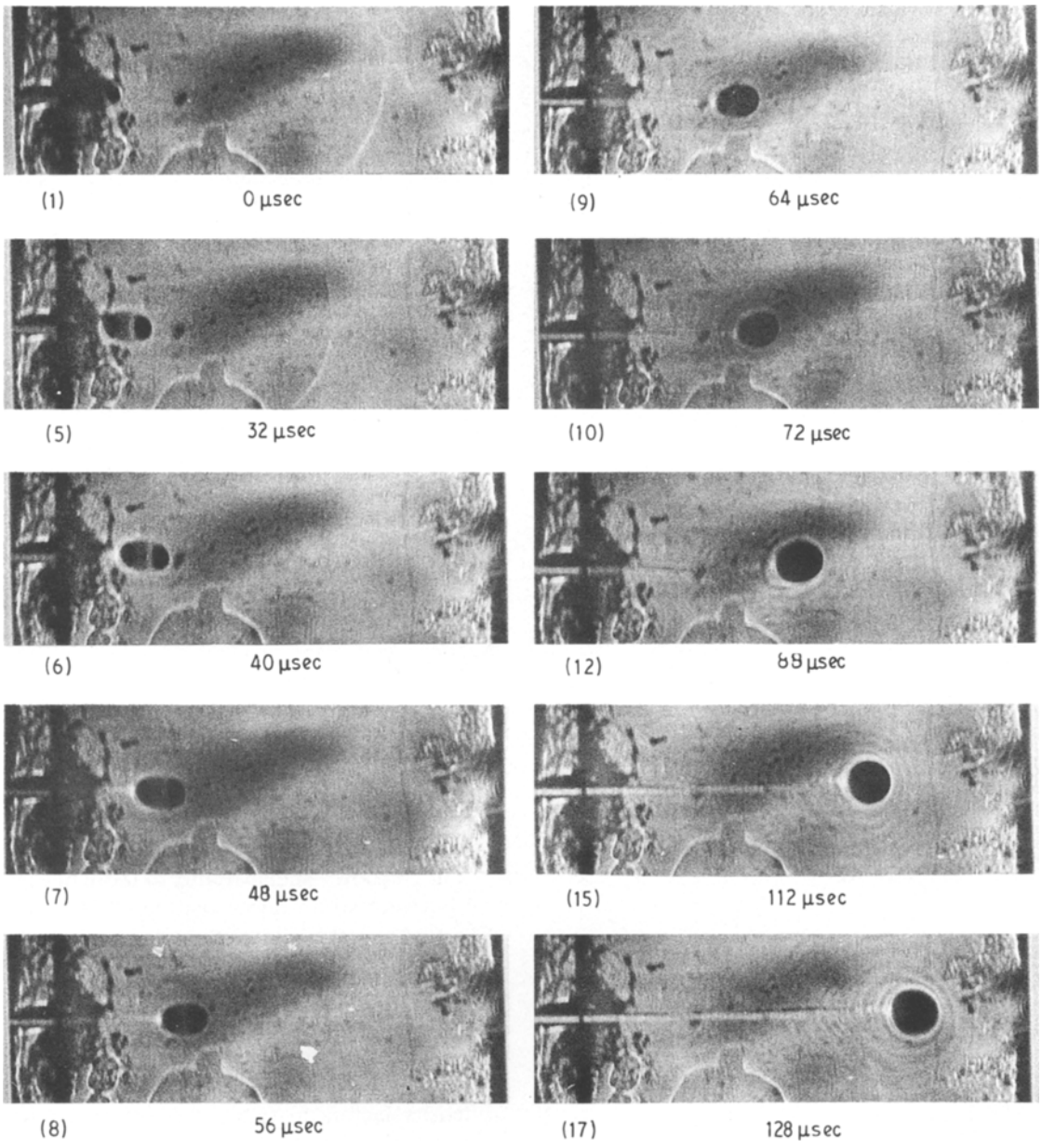

Figure 11 A series of photographs showing the crack propagation in a sandwich specimen with $t_P = 0.001$ m and $t_L = 0.002$ m subjected to a strain rate $\dot{\varepsilon} = 8\ \text{sec}^{-1}$. The two plates were bonded with the adhesive cement trichloroethylene–dichloromethane.

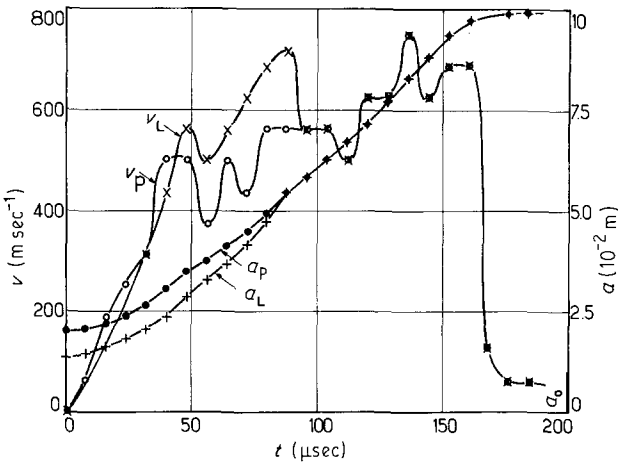

Figure 12 Variation in the velocity, v, and the crack length, a, with time, t, for the specimen in Fig. 11. (○, ●) Plexiglas, (× , +) Lexan.

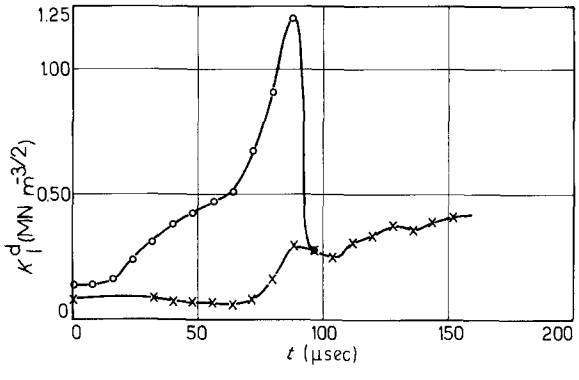

Figure 13 Variation in K_I^d with time, t, for the specimen in Fig. 11. (○) Plexiglas, (×) Lexan.

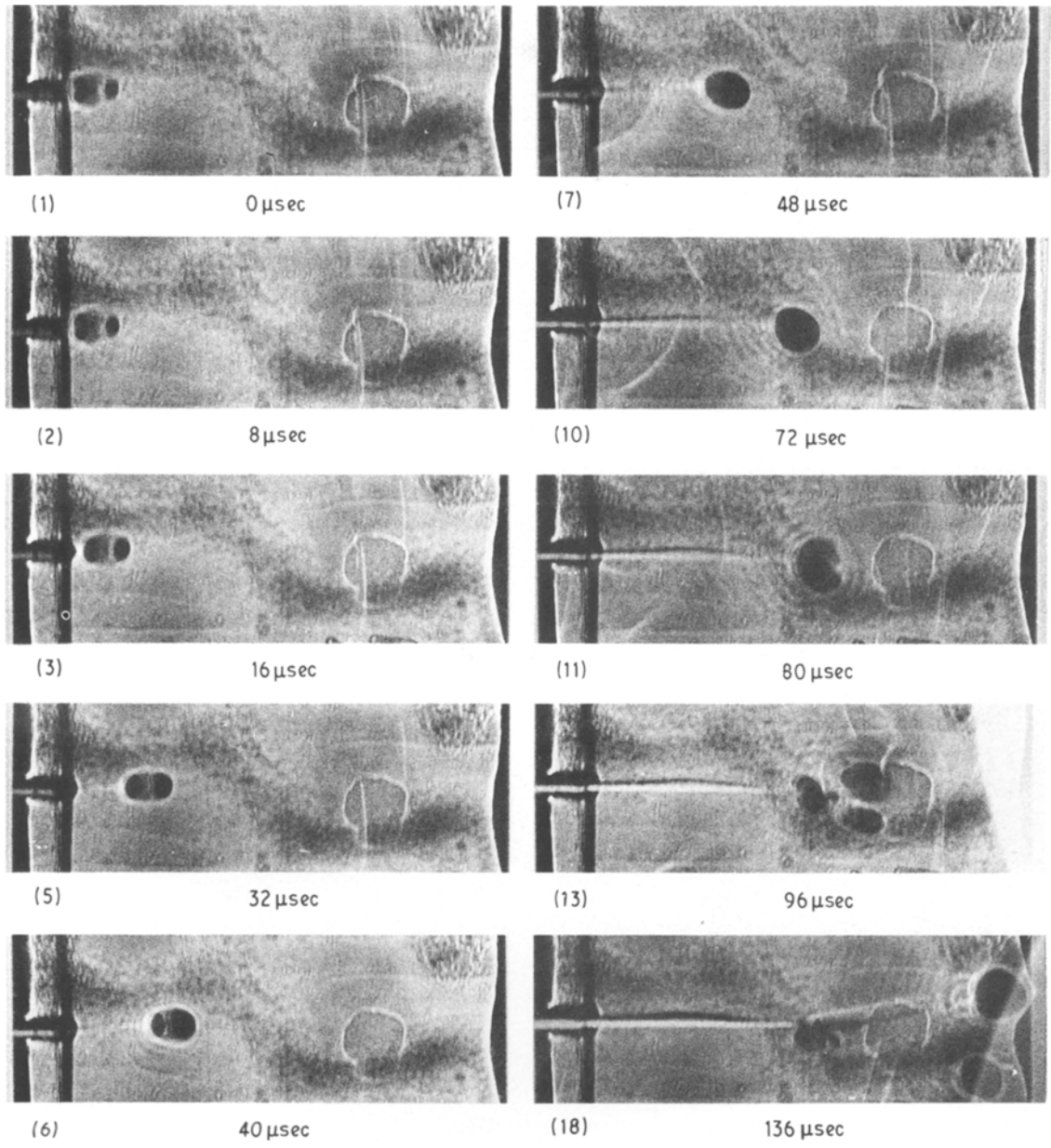

Figure 14 A series of photographs showing the crack propagation in a sandwich specimen with $t_P = 0.001$ m and $t_L = 0.002$ m subjected to a strain rate $\dot{\varepsilon} = 24\ \text{sec}^{-1}$. The two plates were bonded with the adhesive cement trichloroethylene–dichloromethane.

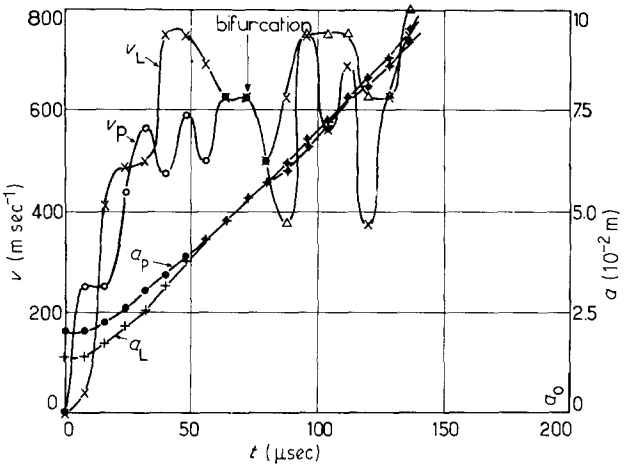

Figure 15 Variation in the velocity, v, and the crack length, a, with time, t, for the specimen in Fig. 14. (○, ●) Plexiglas, (× , +) Lexan.

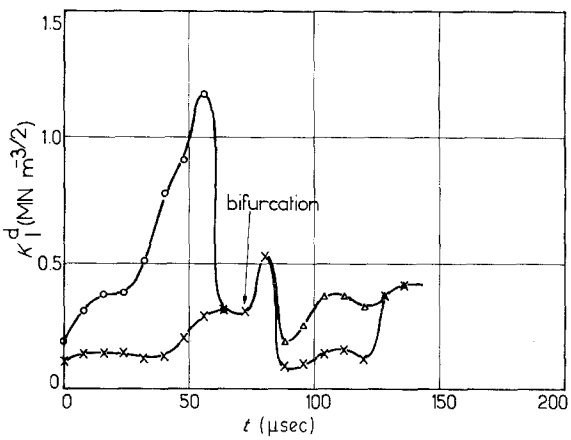

Figure 16 Variation in K_I^d with time, t, for the specimen in Fig. 14. (○) Plexiglas, (× , △) Lexan.

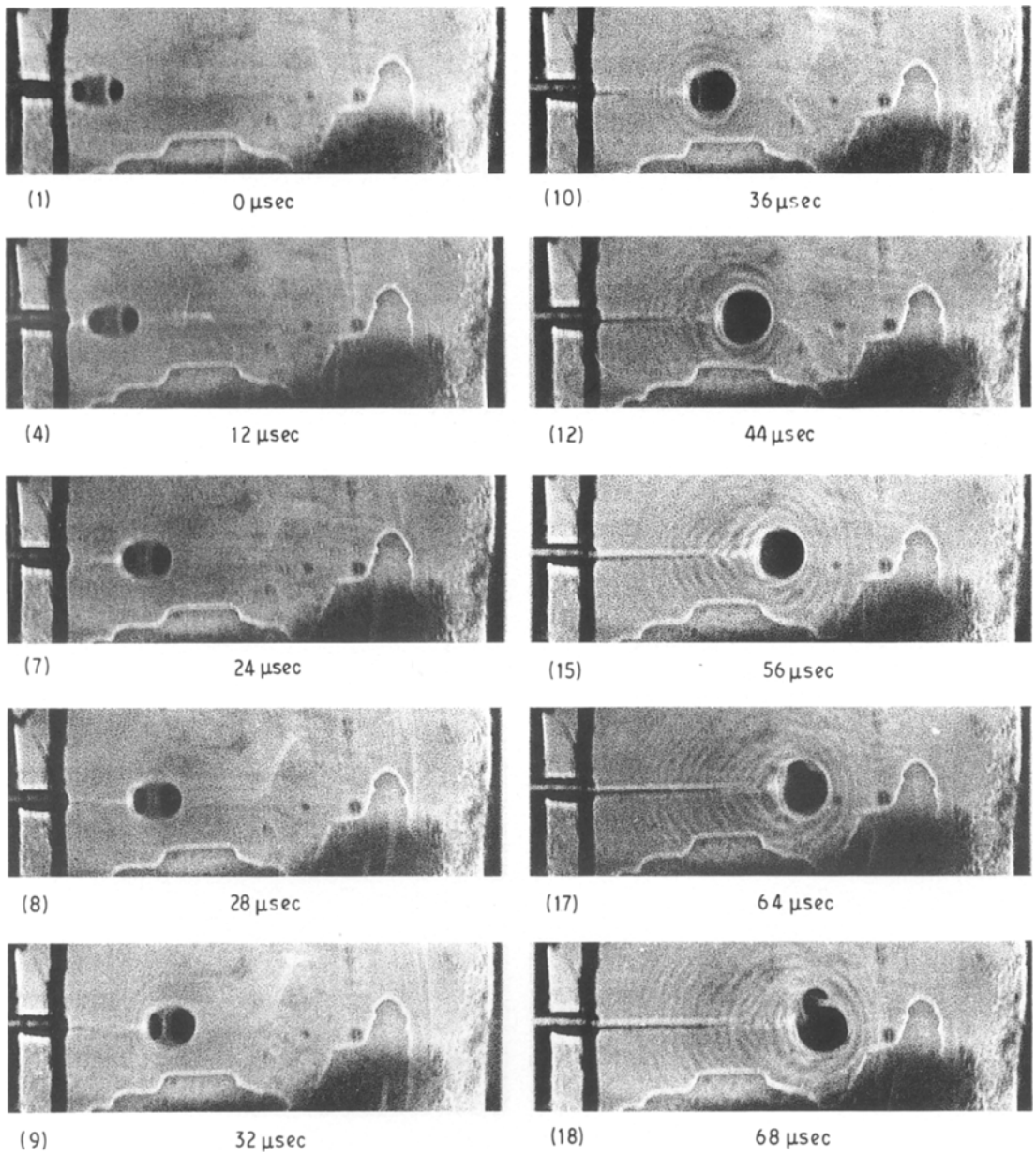

Figure 17 A series of photographs showing the crack propagation in a sandwich specimen with $t_P = 0.001$ m and $t_L = 0.002$ m subjected to a strain rate $\dot{\varepsilon} = 40\,\text{sec}^{-1}$. The two plates were bonded with the adhesive cement trichloroethylene–dichloromethane.

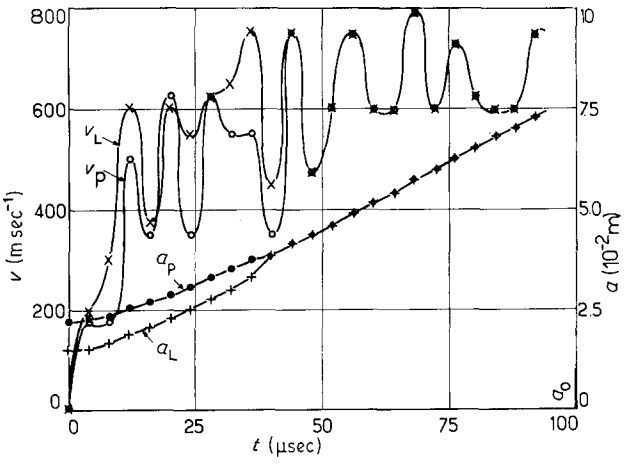

Figure 18 Variation in the velocity, v, and the crack length, a, with time, t, for the specimen in Fig. 17. (○, ●) Plexiglas, (× , +) Lexan.

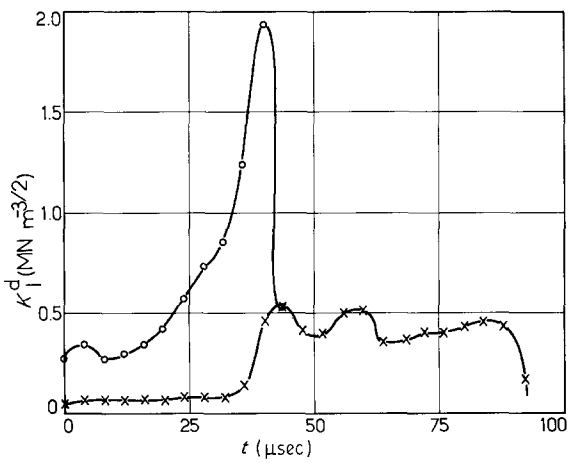

Figure 19 Variation in K_I^d with time, t, for the specimen in Fig. 17. (○) Plexiglas, (×) Lexan.

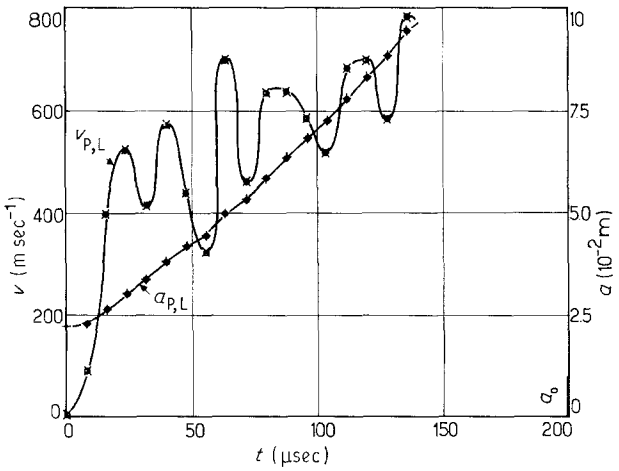

Figure 20 Variation in the crack velocity, v, and the crack length, a, in a sandwich specimen with $t_P = 0.001$ m and $t_L = 0.001$ m subjected to a strain rate $\dot{\varepsilon} = 4\ \text{sec}^{-1}$. The two plates were bonded with the adhesive cement trichloroethylene–dichloromethane. (○, ●) Plexiglas, (× , +) Lexan.

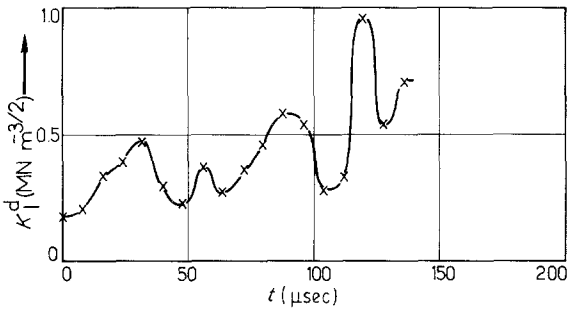

Figure 21 Variation in K_I^d with time, t, for the specimen in Fig. 20. (×) Lexan.

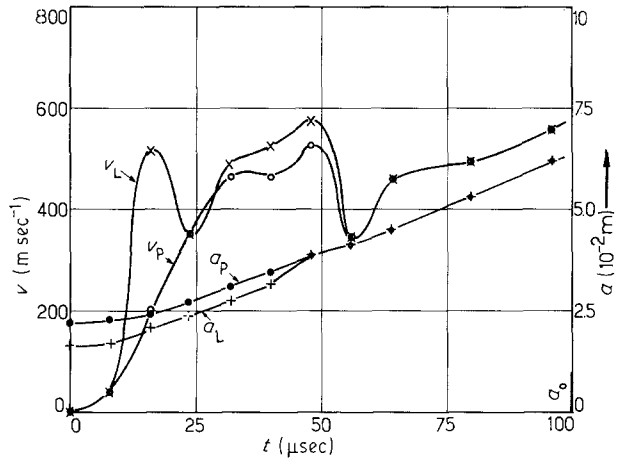

Figure 22 Variation in the crack velocity, v, and the crack length, a, in a sandwich specimen with $t_P = 0.001$ m and $t_L = 0.001$ m subjected to a strain rate $\dot{\varepsilon} = 8\ \text{sec}^{-1}$. The two plates were bonded with the adhesive cement trichloroethylene–dichloromethane. (○, ●) Plexiglas, (× , +) Lexan.

Figs 24 and 25 present the variation of crack velocities, crack lengths and stress intensity factor, respectively, for similar sandwich specimens but with strain rate $\dot{\varepsilon} = 24\ \text{sec}^{-1}$. Similar results can be observed as in the previous specimen in comparison with those in Figs 15 and 16 but the coincidence time of the two cracks is $t_{coin} \simeq 30$ μsec (shorter than those in Fig. 14).

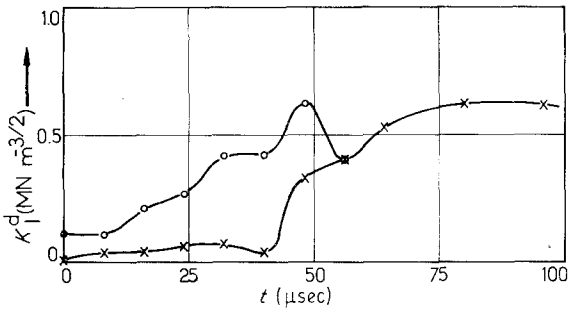

Figure 23 Variation in K_I^d with time, t, for the specimen in Fig. 22. (○) Plexiglas, (×) Lexan.

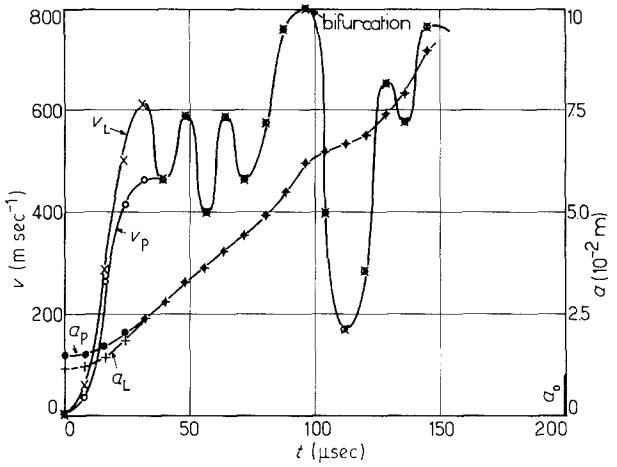

Figure 24 Variation in the crack velocity, v, and the crack length, a, in a sandwich specimen with $t_P = 0.001$ m and $t_L = 0.001$ m subjected to a strain rate $\dot{\varepsilon} = 24\ \text{sec}^{-1}$. The two plates were bonded with the adhesive cement trichloroethylene–dichloromethane. (○, ●) Plexiglas, (× , +) Lexan.

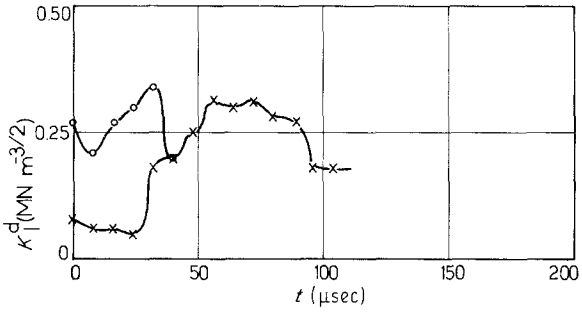

Figure 25 Variation in K_I^d with time, t, for the specimen in Fig. 24. (○) Plexiglas, (×) Lexan.

Finally, Figs 26 and 27 show the variation of crack velocities, crack lengths and stress intensity factor, respectively, for similar sandwich specimens but with strain rate $\dot{\varepsilon} = 40\ \text{sec}^{-1}$. It can be observed that the time lag is zero as in Figs 20 and 21, and the values of the velocities and stress intensity factor in comparison with those in Figs 18 and 19 remain smaller than those.

Fig. 28 shows the variation of coincidence time, t_{coin}, with the strain rate, $\dot{\varepsilon}$, for sandwich specimens with thickness of the plates $t_P = t_L$ and $t_L = 2t_P$. It can be observed that for sandwich specimens fractured with the same strain rate, t_{coin} is longer for the sandwich specimens with $t_L = 2t_P$ than in the sandwich with $t_P = t_L$.

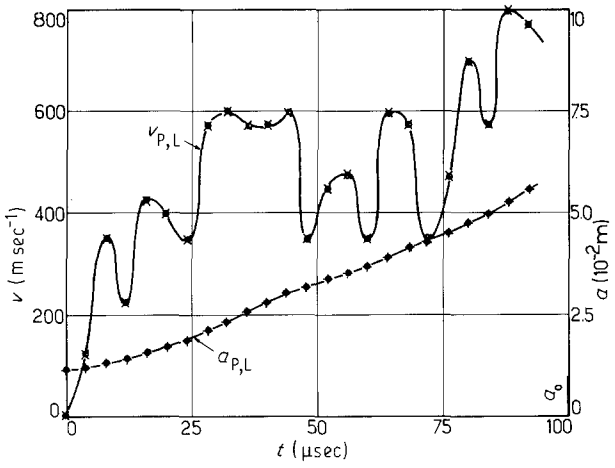

Figure 26 Variation in the crack velocity, v, and the crack length, a, in a sandwich specimen with $t_P = 0.001$ m and $t_L = 0.001$ m subjected to a strain rate $\dot{\varepsilon} = 40\,\text{sec}^{-1}$. The two plates were bonded with the adhesive cement trichloroethylene–dichloromethane. (○, ●) Plexiglas, (× , +) Lexan.

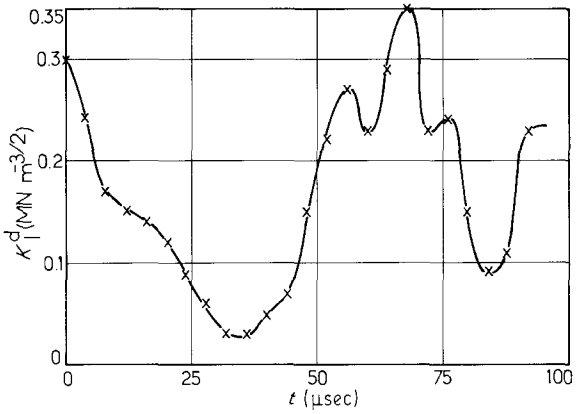

Figure 27 Variation in K_I^d with time, t, for the specimen in Fig. 26. (×) Lexan.

5. Conclusions

The following phenomena were observed during crack propagation in sandwich plates.

1. Debonding of the phases takes place. The degree of debonding depends on the adhesion between the two phases which in turn depends on the adhesive used.

2. There is a time lag between crack initiation in the two phases which depends on the nature of the phases and their degree of compatibility. This time lag decreases as the strain rate increases.

3. The two cracks met after a time which depends on the thickness of the phases and on the strain rates.

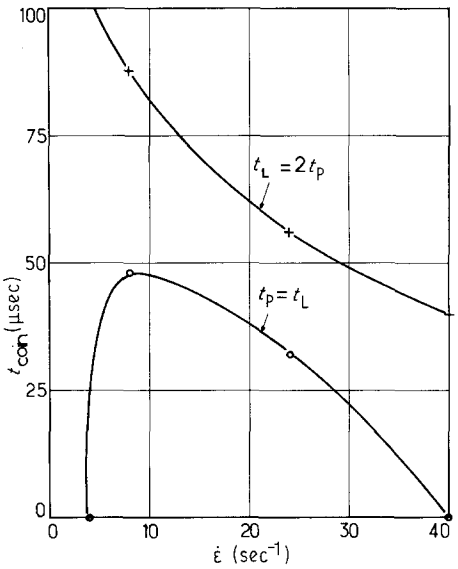

Figure 28 Variation in the time of coincidence t_{coin} of the two cracks with strain rate, $\dot{\varepsilon}$.

So, the coincidence time, t_{coin}, decreases as the strain rate increases. Also, t_{coin} decreases as the thickness, t_L, of the ductile phase, decreases, and t_{coin} is shorter for sandwich specimens with $t_P = t_L$ than for the sandwich with $t_L = 2t_P$.

4. The values of the velocities of the two propagating cracks and the stress intensity factor for the sandwich with $t_P = t_L$, mainly up to the time at which the two cracks meet, remain smaller than the respective values of the sandwich with $t_L = 2t_P$.

References

1. F. ERDOGAN and K. ARIN, *Engng Fract. Mech.* **4** (1972) 449.
2. P. C. Y. LEE and N. CHANG, *J. Elasticity* **9** (1979) 51.
3. P. S. THEOCARIS and G. A. PAPADOPOULOS, *Engng Fract. Mech.* **13** (1980) 683.
4. *Idem*, ASTM STP 791, Vol. 2 (American Society for Testing and Materials, Philadelphia, Pennsylvania, 1983) pp 320–37.
5. A. J. ROSAKIS, *Engng Fract. Mech.* **13** (1980) 331.
6. A. J. ROSAKIS and A. T. ZEHNDER, *J. Elasticity* **15** (1985) 347.
7. P. S. THEOCARIS and G. A. PAPADOPOULOS, *Materialprüfung* **22** (1980) 246.
8. *Idem, J. Strain Analy.* **16** (1981) 29.
9. D. RAFTOPOULOS, D. KARAPANOS and P. S. THEOCARIS, *J. Phys. D Appl. Phys.* **9** (1976) 869.

Received 11 August 1989
and accepted 19 February 1990